J Nanotechnol Nanomaterials. 2024;5(1):31-45.

Journal of Nanotechnology and Nanomaterials Research Article

Biosynthesis of Manganese Dioxide Nanoparticles and Optimization of Reaction Variables

Abelneh Terefe Mekuria[1,*]

[1]Department of Chemical Engineering, College of Biological and Chemical Engineering, Addis Ababa Science and Technology University, Addis Ababa, P.O. Box 16417, Ethiopia

[*]Correspondence should be addressed to Abelneh Terefe Mekuria, kalabel0941@gmail.com

Received date: March 25, 2024, **Accepted date:** April 30, 2024

Citation: Mekuria AT. Biosynthesis of Manganese Dioxide Nanoparticles and Optimization of Reaction Variables. J Nanotechnol Nanomaterials. 2024;5(1):31-45.

Abstract

Biosynthesis is an efficient and environmentally friendly process used to synthesize nanoparticles. This study presents a simple, environmentally friendly, and cost-effective method for synthesizing manganese dioxide nanoparticles from aqueous manganese (II) acetate using lemon extract as a reducing agent. Turmeric extract (curcumin) was employed to stabilize the biosynthesized nanoparticles. UV-visible spectroscopy was used to evaluate the concentration of nanoparticles at 350 nm wavelength. The scanning electron microscope verified that the nanoparticles had a rod-like shape. Fourier's transform infrared spectroscopy revealed an absorption peak at 558 cm^{-1}, which corresponded to the stretching vibration of O-Mn-O. Response surface methodology, namely the central composite design, was employed to optimize reaction variables such as temperature, pH, and lemon extract ratio during the synthesis. These variables were optimized by measuring the absorption intensity of nanoparticles at 350 nm with UV-visible spectroscopy. The optimal values were claimed to be a lemon extract ratio of 75%, a temperature of 50°C, and a pH of 3.4. The lemon extract ratio was found to be a viable variable that determines the formation of nanoparticles, followed by temperature and pH. Hence, the utilization of sustainable plant extracts enhances the synthesis of nanoparticles without actual effects on the environment. MnO_2 nanoparticles are used in a variety of applications, including energy storage, photocatalysis, adsorbents, sensors, and detectors for a wide range of biomedical molecules.

Keywords: Biosynthesis, Manganese dioxide nanoparticles, Lemon extract, Curcumin, Optimization, Response surface methodology, Central composite design

Introduction

Recent advances in nanotechnology have led to a variety of research areas focusing on nanoparticles [1-3]. Scientists have been looking at green nanotechnology and novel materials to improve human living standards. Nanomaterials have been extensively exploited in several fields of study, including environmental remediation, renewable and clean energy production and storage, optical applications, and sustainability [4-8]. With the capability of photocatalytic oxidation, nanoparticles can decompose organic compounds in water and air under sustainable energy (sunlight) [9]. Other classes of nanomaterials are good electrochemical sensors and contribute advantages such as short detection times, ease of operation, simplified pretreatment, and low cost over traditional measurement techniques [10]. Furthermore, nanoparticles have a higher specific surface area and so offer outstanding properties in the fields of energy storage, optics, biological compatibility, and the minimization of defects [11,12]. Manganese-based nanomaterials are receiving interest among the diverse nanomaterials because of their particular qualities such as chemical stability, environmental compatibility, and electrochemical activity [13]. MnO_2 nanoparticles are versatile materials with a wide range of applications such as energy storage, environmental purification, catalysis, biomedicine, and sensors [13-16].

Various conventional methods have been used in the synthesis of nanomaterials, including sol-gel, solvothermal, pyrolysis, high-energy irradiation, electrochemical deposition, photo-induced reduction, hydrothermal, and electrochemical reduction [17-20]. Conventionally, manganese-based

nanomaterials have been produced by oxidizing Mn (II) in a basic solution or reducing permanganate [21,22]. However, these methods are not environmentally friendly as they consume more energy, produce organic solvents, generate intermediate chemicals, and emit toxic by-products into the environment [23]. The green chemistry-based syntheses of nanomaterials have gained popularity due to their environmentally friendly, low cost, ease of use, less toxic by-products, less time consumption, performance at ambient temperature and pressure, and ease of scale-up [24]. The biosynthesis of nanomaterials is increasingly significant in science due to the rapidly growing awareness of the risks generated by the conventional syntheses of nanoparticles [25,26]. The biosynthesis of nanoparticles utilizes bacteria [27], algae [28], fungi [29], and plants [30]. Among the biological materials listed, plant extract-based biosynthesis has attracted research interest due to its large-scale nanoparticle synthesis. Plant extracts have a variety of phytochemicals that have important roles as reducing agents and stabilizers and are therefore more suitable than synthesis with microorganisms [21]. In addition, the antioxidant properties of plant extracts play a greater role in the synthesis of nanoparticles. The extracts obtained from *Jatropha curcas, Azadirachta indica* [31], *Dittrichia graveolens (L.), Coriandrum sativum* [32], *Polyalthia longifolia, Euphorbia hirta* [24], *Parthenium* [33], and many others provide the principle of biosynthesis that are environmentally friendly. Lemon extract (*Citrus limon*), which is rich in citric and ascorbic acid was used as a reducing agent for the synthesis of nanoparticles [34,35]. In addition, it contains various bioactive compounds including flavonoids, ascorbic acid, phenolic compounds, and carotenoids [36-39]. Various studies have proven that *Citrus limon* contributes various health benefits to humans in terms of anti-oxidative, antibacterial, anti-inflammatory, and anti-tumor properties [40,41]. The other plant extract called curcumin has been used as a stabilizing agent for nanoparticles [42].

This study was focused on the biosynthesis of MnO_2 nanoparticles utilizing lemon extract to reduce manganese ions and curcumin to stabilize the nanoparticles. The other focus was on optimizing the reaction variables involved in nanoparticle synthesis using Response Surface Methodology (RSM), namely Central Composite Design (CCD).

Materials and Methods

Manganese (II) acetate [$(CH_3COO)_2Mn{\cdot}4H_2O$] ≥ 99%, analytical grade, was purchased from Sigma-Aldrich, USA. Lemon fruits and turmeric roots were purchased from a vegetable market in Addis Ababa, Ethiopia. Sodium hydroxide (NaOH), nitric acid (HNO_3), and ethanol (95%) were purchased from General Chemicals and Trading plc, Addis Ababa, Ethiopia. Distilled water was used to prepare an aqueous manganese (II) acetate solution. A VENOR 150 g commercial spice grinder (with a mesh size of 40-200) was used to grind the turmeric roots to a powder. A multifunctional lemon juicer was used to extract lemon juice from lemon fruits. UV-visible spectroscopy (Shimadzu: UV-1800), Fourier's transform infrared spectroscopy (Nicolet iS50, USA), and field emission scanning electron microscope (FEI, Inspect F50) were employed to characterize MnO_2 nanoparticles.

Preparation of extracts

Lemon fruits were thoroughly washed with distilled water and then cut into smaller pieces. Subsequently, these smaller lemon pieces were squeezed using the multifunctional lemon juicer to obtain the extract. The extract was filtered with filter paper (Whatman's No.1). The filtrate was collected and stored in a refrigerator at 4°C. The turmeric roots were also properly washed with distilled water, chopped into pieces using a knife, and sun-dried for three days. The turmeric roots were then processed into a 100-mesh powder. 15 g of turmeric powder was added to an Erlenmeyer flask containing 300 ml of 95% ethanol and heated for 5 minutes. The mixture was cooled and then centrifuged in batches for about 15 minutes at 8,000 rpm [43]. Finally, the supernatants (curcumin) were collected in a clean polyethylene bottle and stored in a refrigerator at 4°C.

Biosynthesis of MnO_2 nanoparticles

The biosynthesis of MnO_2 nanoparticles was performed via the utilization of lemon extract as a reducing agent and curcumin as a stabilizing agent. One millimole of manganese acetate (II) aqueous solution was prepared for the synthesis. The prepared manganese acetate aqueous solution was placed into a clean beaker and heated with a magnetic stirring plate. The lemon extract was progressively mixed into the manganese acetate aqueous solution while stirring. The mixture was stirred for 1 hour. To stabilize the nanoparticles, curcumin was added to a beaker containing a mixture and allowed to stir again for 1 hour. Then, the samples were centrifuged at 8,000 rpm for 15 min and then washed with distilled water and ethanol several times [43]. Following centrifugation, the resultant precipitations were collected and then dried in a water bath at 40°C [44]. The effects of the reaction variables such as temperature, pH, and lemon extract ratio were investigated and presented in a statistical experimental design (Section "Statistical experimental design"). The overall procedure for the biosynthesis technique is shown in **Scheme 1**.

The proposed reaction mechanism

Several research studies rely on the biomolecules that power the environmentally friendly synthesis of nanoparticles. However, the nature of the reaction between ionic compounds and biological extracts is not entirely well understood. Manganese ions (Mn^{2+}) are generated in an aqueous solution of manganese (II) acetate [$(CH_3COO)_2 Mn{\cdot}4H_2O$]. When the lemon extract is allowed to mix with the aqueous solution of manganese acetate, manganese metal ions begin to reduce

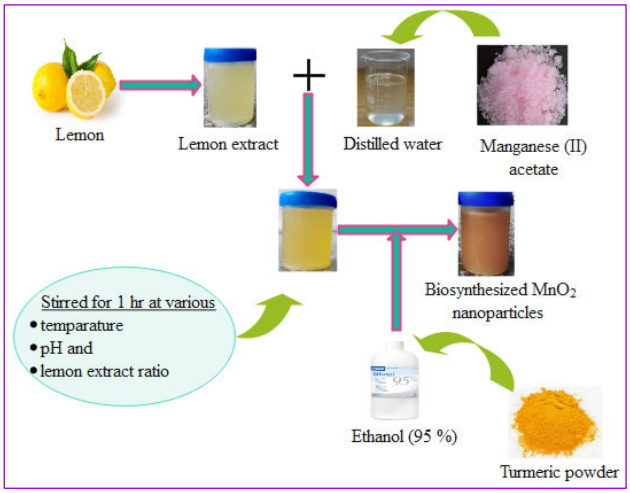

Scheme 1. Preparation procedure for MnO_2 nanoparticles. From the Figure, MnO_2 nanoparticles were synthesized from aqueous manganese (II) acetate solution. Lemon extract was utilized to reduce manganese ions and Turmeric extract (curcumin) was used to stabilize the nanoparticles. Ethanol (95%) was used to extract curcumin from turmeric roots. Wondershare EdrawMax was employed to generate this figure.

into manganese metal atoms. The reduced manganese atoms may combine with oxygen originating from the atmosphere or degraded phytochemicals to form MnO_2. Subsequently, MnO_2 tends to link with each other through electrostatic attraction to form MnO_2 nanoparticles. The phytochemicals from curcumin stabilize the nanoparticles by preventing agglomeration.

Characterization of MnO_2 nanoparticles

A UV-visible spectrophotometer was used to identify the formation of MnO_2 nanoparticles at a wavelength of 350 nm. FT-IR (Nicolet iS50, USA) spectral study was utilized to determine the biomolecules based on the changes in the functional groups found in the sample, including the nanoparticles. It was investigated at a wavelength ranging from 475 to 4,000 cm^{-1}. FESEM (FEI, Inspect F50) was employed to investigate the surface morphology of the MnO_2 nanoparticles. The samples containing the nanoparticles were mounted on aluminum stubs with conductive carbon tape and scanned.

Optimization of reaction variables

Statistical analysis: The optimization strategy in the synthesis of MnO_2 nanoparticles serves to find the best experimental conditions to achieve a stable result [45]. RSM is a statistical method in which quantitative data from experiments is used to create regression model equations and operating conditions [46]. This can be done by performing a preliminary screening design to predict which of the experimental reaction variables and their interactions have significant effects on the synthesis. RSM is a group of statistical techniques used to define the relationship between input variables and reaction responses. It is usually used to justify the relationship between input variables and reaction responses, to determine the significance of the different variables, and to predict the optimal values that provide maximum product yield.

Statistical experimental design: Among the statistical experimental design techniques, the response surface

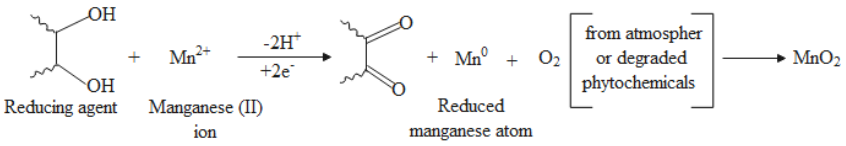

Scheme 2. Shows the proposed reaction mechanism for the biosynthesis of MnO_2 nanoparticles. In this regard, lemon extract was employed to reduce Mn^{2+} to Mn. The reduced Mn then reacted with oxygen obtained from the degradation of phytochemicals in the extracts or from the air to form MnO_2. Due to the electrostatic attraction, MnO_2 tends to combine to form nanoparticles.

method was selected to study the effects of the main variables and their interactions. The CCD is one of the most commonly utilized experimental design methods within RSM. It provides additional extreme values by overshooting the given values of variables and offers a good-quality prediction of the interaction effects [47]. Moreover, the significance of CCD is to generate a second-order model that contains the interacting terms that provide information on the correlation of the reaction variables with each other [48]. In the optimization study, the volume ratios (50%, 62.5%, and 75%) of lemon extract to one millimole of manganese (II) acetate aqueous solution at various pH values (3, 3.5, and 4) were mixed for 1 hour at different temperatures (50°C, 55°C, and 60°C) under a hot plate of a magnetic stirrer. After 1 hour of stirring, 20 ml of curcumin was added to the beaker containing the mixture, and stirring was continued for 1 hour. The pH of the reaction was adjusted with 10% NaOH or 10% HNO_3 [32]. Based on the CCD method, 20 experiments with two levels were designed using Design Expert 12 software. The actual values of each run were taken to optimize the effect of temperature, pH, and lemon extract ratio on the synthesis, as shown in **Table 1**. These actual values were recorded by measuring the absorption intensity using a UV-visible spectrophotometer (Shimadzu: UV-1800). The samples were scanned in the wavelength range of 200 to 1000 nm to investigate the optical absorption spectra of MnO_2 nanoparticles.

Results and Discussion

Characterization of MnO_2 nanoparticles

UV-visible spectral analysis of MnO_2 nanoparticles: The formation of MnO_2 nanoparticles was detected using a UV-visible spectrophotometer. The absorption intensity of nanoparticles detected with UV-visible spectroscopy depends on the concentration of nanoparticles in the sample solution. An increased concentration of the nanoparticles in the sample can desirably enhance the absorption intensity

Table 1. Experimental setup using CCD for the synthesis of MnO_2 nanoparticles and absorption intensity. The reaction variables of lemon extract ratios (50%, 62.5%, 75%), pH of (3, 3.5, 4), and temperatures of (50°C, 55°C, 60°C) were designed using Design Expert 12 software. Based on the central composite design 20 runs of experiments were conducted as shown in the table to investigate the effects of these variables on MnO_2 nanoparticles.

Run	A: Temperature, °C	B: pH	C: Lemon extract ratio, %	Absorbance intensity at 350 nm	
				Actual value	Predicted value
1	55	3.5	62.5	1.012	1.012
2	55	3.5	62.5	1.079	1.012
3	60	4	75	0.865	0.806
4	55	3.5	62.5	1.109	1.012
5	55	3.5	62.5	0.995	1.012
6	60	4	50	0.715	0.658
7	55	3.5	41.5	0.826	0.802
8	46.6	3.5	62.5	1.195	1.100
9	60	3	50	0.783	0.763
10	55	3.5	62.5	1.028	1.012
11	60	3	75	0.947	0.878
12	50	4	75	1.123	1.074
13	63.4	3.5	62.5	0.854	0.832
14	55	2.7	62.5	0.772	0.696
15	50	3	75	1.147	1.133
16	50	4	50	0.718	0.717
17	50	3	50	0.821	0.810
18	55	4.3	62.5	0.602	0.558
19	55	3.5	83.5	1.297	1.199
20	55	3.5	62.5	1.107	1.021

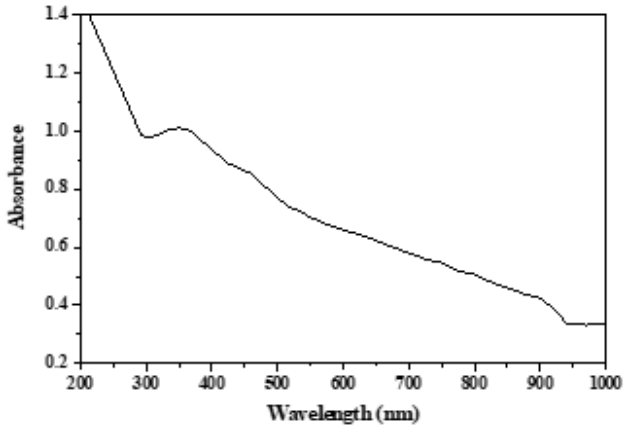

Figure 1. Depicts a UV-visible spectrum of MnO_2 nanoparticles conducted in the author's former published article [35]. A UV-visible spectrophotometer (Shimadzu: UV-1800) was utilized and the samples were scanned in the wavelength ranging from 200 to 1,000 nm. The optimization of the reaction variables was estimated by recording the absorption intensity at 350 nm.

[49]. In our previous study, the absorbance spectrum of MnO_2 nanoparticles in run 1 (see **Table 1**) is shown in **Figure 1**. The reaction variables involved in this run were a temperature of 55°C, a pH of 3.5, and a lemon extract ratio of 62.5%. The absorption spectrum for this run was detected as a maximal absorption at a wavelength of 350 nm with an absorption peak intensity of 1.012. The absorption intensities of the other runs were determined based on the preset wavelength position of the first experiment. The detection of an absorption band at 350 nm clearly indicates the formation of MnO_2 nanoparticles and is in line with the results reported previously [50].

FESEM analysis of MnO_2 nanoparticles: The surface morphology of MnO_2 nanoparticles synthesized under optimal conditions such as a temperature of 50°C, a pH of 3.4, and a lemon extract ratio of 75% was examined using a scanning electron microscope, as shown in **Figure 2**. The particles are agglomerated and interconnected together to form small clusters. These interconnected clusters in the micron range are generated by the aggregation of phytochemicals and nanoparticles [51]. Previous research demonstrated that the type of aggregation generated by the reducing and capping agents has a significant impact on the surface morphology

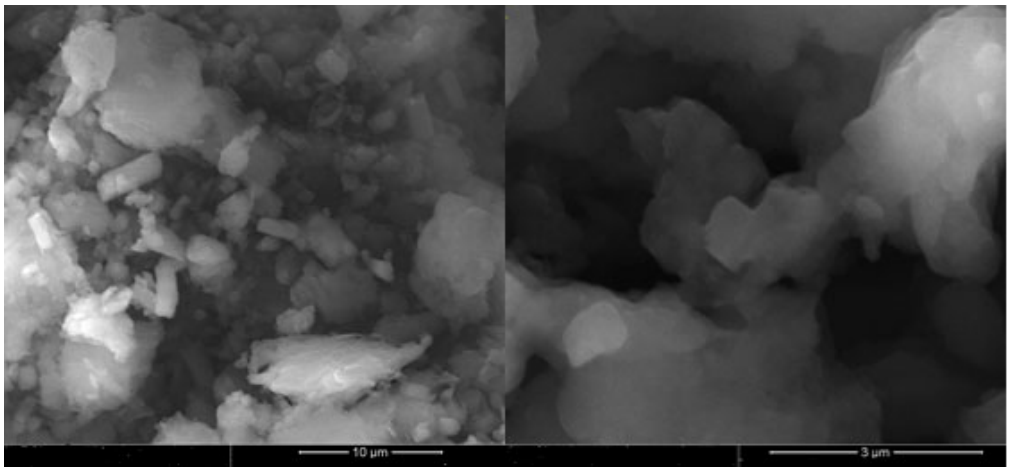

Figure 2. Shows the surface morphology of MnO_2 nanoparticles. A scanning electron microscope (FEI, Inspect F50) was used to show the surface morphology nature of the MnO_2 nanoparticles. The surface morphology was carried out based on the values. A scanning of the optimal reaction variables such as a temperature of 50°C, a pH of 3.4, and a lemon extract ratio of 75%. According to surface morphology, the nanoparticles are agglomerated and interconnected to form clusters in the range of microns.

of MnO_2 nanoparticles, which in turn affects the size and surface area of nanoparticles [52,53]. Because of their long-term affinity, the nanoparticles clump together despite having a larger surface area [54]. Furthermore, environmental variables may influence the spontaneous aggregation of nanoparticles into asymmetrical clusters [55]. The developed MnO_2 nanoparticles have appeared to be rod-shaped and are in good agreement with previous findings [56].

FT-IR analysis of MnO_2 nanoparticles: Figure 3 depicts the FT-IR spectra of MnO_2 nanoparticles synthesized at the optimal variables. The spectrum band detected at 3270 cm^{-1} shows the phenolic hydroxyl group (-OH) found in the phytochemicals. The peak detected at 2930 cm^{-1} is due to the presence of carbon-hydrogen stretching. The band shown at 1590 cm^{-1} is related to the C = C stretching vibration of aromatic compounds [57]. The peaks found at 1435 cm^{-1} and 1265 cm^{-1} correspond to C-H and C-H, respectively. A significant peak appeared at 1032 cm^{-1} is attributed to C-O in flavones, polysaccharides, and terpenoids that are largely found in plant extracts used as reducing and capping agents in the synthesis process, as reported in the literature [58]. These plant extract components play a greater role in manganese ion reduction and stabilization, which prevent the accumulation of nanoparticles together. The peaks that are detected in the range of 1400–1000 cm^{-1} are due to the Mn-OH surface [59]. FT-IR detected the bio-organic compounds such as alkaloids, flavonoids, and phenols found in the lemon extract that are essential in the manganese metal reduction, as reported in [60]. The absorption intensity peak at 558 cm^{-1} is ascribed to the stretching vibration of O-Mn-O that confirms the presence of MnO_2 nanoparticles, and it is in agreement with the previously studied literature [59,61,62].

The effect of reaction variables on MnO_2 nanoparticles

Temperature, plant extract, and pH are crucial variables that must be optimized to synthesize nanomaterials [63]. In this study, a high lemon extract ratio (75%) has favored the formation of MnO_2 nanoparticles and is in line with the previous documented work [34]. In another study, a high concentration of lemon extract with the precursor solution 4:1 (lemon extract: $AgNO_3$) favored the synthesis of silver nanoparticles [64]. This may be attributed to the presence of phytochemical components such as ascorbic acid and phenolic compounds in lemon extract that can efficiently reduce metal ions to form nanoparticles [65]. The increased number of reducing species in lemon extract, particularly ascorbic acid, and citric acid, are associated with carboxylic functional groups, while proteins and free amino acids are associated with the amine group (N–H), which are all rich in lemon extract [66]. The three-carboxylate groups existing in citric acid enabled lemon extract to generate stable metal ion complexes. To control the size and morphology of a wide spectrum of nanoparticles, researchers have utilized citric acid as a reducing and stabilizing agent [66,67]. In addition, some authors reported that a low concentration of lemon extract in the precursor solution 1:9 (lemon extract: $AgNO_3$) was preferred for the synthesis of silver nanoparticles [68]. However, the author suggests that a sufficient concentration of biomolecules is essential for the efficient conversion of metal ions into nanoparticles. A polyphenolic compound that exists in curcumin has a relatively high stability potential for nanoparticle synthesis. There is evidence for the efficient stability performance of nanoparticles via the utilization of curcumin [69,70].

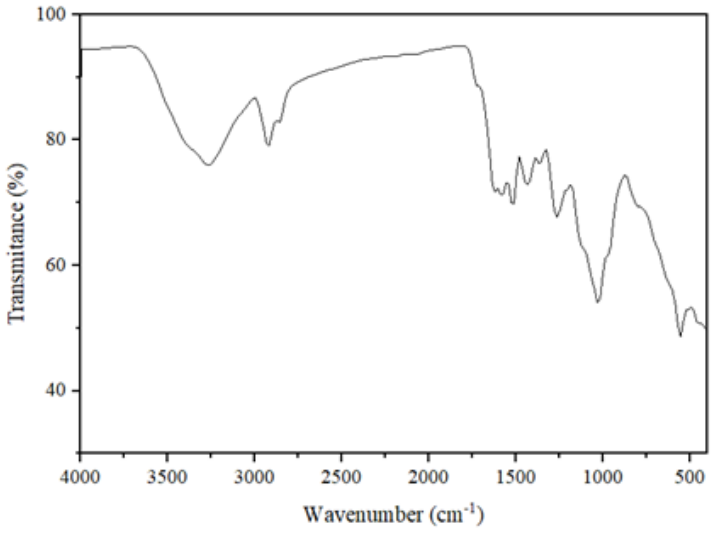

Figure 3. The different functional groups originating from the extracts and the formation of nanoparticles in the samples were investigated using Fourier transform infrared spectroscopy (Nicolet iS50, USA). According to this investigation, the MnO_2 nanoparticles are detected at 558 cm^{-1}.

Temperature is another important variable in the synthesis of nanoparticles. The effect of temperature in this study was investigated by considering temperature values ranging from 46.5°C to 63.4°C. In this regard, the optimal temperature of 50°C was found to be effective for the formation of nanoparticles, a similar result was obtained by the previous work [71]. However, at a very low temperature, the synthesis of nanoparticles cannot be achieved, as evidenced by silver nanoparticle synthesis at 5°C [72]. The biomolecules engaged in the reduction of the metal precursor's ion may have a higher kinetic energy when the reaction temperature rises, and this enhances the consumption of metallic ions more quickly. Most biosynthesis techniques are carried out at room temperature, as reported in some literature [73,74]. In another study, *Hygrophila spinosa* extract-mediated synthesis of gold nanoparticles was found to be ineffective at room temperature, as reported [75]. On the contrary, some authors reported nanoparticle synthesis even at higher temperatures (70°C) [44]. Furthermore, using the extract of *Hygrophila spinosa*, gold nanoparticles were synthesized at a reaction temperature of 80°C [75]. I suggest that higher temperatures may deactivate the phytochemical compounds that are responsible for the metal ion reduction and stabilization of the nanoparticles.

The activity levels of biomolecules used in the biosynthesis of nanoparticles can vary depending on the pH of the reaction medium. In this study, a pH of around 3.4 was found to be the optimal value. A similar pH value was obtained in the study of manganese nanoparticle synthesis using lemon extract [57]. The pH value is found in the acidic medium due to the presence of ascorbic and citric acids in lemon extract. In the study of manganese dioxide green synthesis via *Yucca gloriosa* leaf extract, the optimum pH value was 6 [76]. In another study of manganese dioxide nanoparticle green synthesis using *Malpighia emarginata* leaf extract, the pH of the reaction medium was found to be 11 [77]. Therefore, it can be concluded that the adjustment of pH may vary depending on the type of plant extract utilized and the alkalinity of the precursor solutions involved in the process of nanoparticle synthesis.

Statistical analysis

Analysis of variance: The absorption intensities calculated using the model equation and the corresponding measured experimental absorption values agree well, as shown in **Table 2**. In addition, there is good agreement between the measured and predicted response values, as indicated by the closeness between R^2 (0.9669) and the fitted R^2 (0.9370) shown in **Table 3**. This means that the predicted values are closer to the actual values, and the quadratic polynomial model is therefore of great importance for the prediction of the experimental variables [78,79]. The signal-to-noise ratio was determined using Adeq precision and is greater than 4, which indicates the

Table 2. Variance analysis of the quadratic model for the synthesis of MnO_2 nanoparticles. As shown in the Table, the Prob. > F value of a model is less than 0.05 revealing that the model including the individual variables is statistically significant.

Source	Sum of square	Df	Mean square	F value	P-value Prob >F	
Model	0.6486	9	0.0721	32.41	<0.0001	Significant
A: temperature (°C)	0.0842	1	0.0842	37.88	0.0001	
B: pH	0.0232	1	0.0232	10.43	0.0090	
C: lemon extract ratio (%)	0.2503	1	0.2503	112.57	<0.0001	
AB	0.0001	1	0.0001	0.0297	0.8665	
AC	0.0217	1	0.0217	9.78	0.0108	
BC	0.0005	1	0.0005	0.2375	0.6365	
A^2	0.0040	1	0.0040	1.80	0.2099	
B^2	0.2664	1	0.2664	119.82	<0.0001	
C^2	0.0001	1	0.0001	0.0350	0.8553	
Residual	0.0222	10	0.0022			
Lack of Fit	0.0099	5	0.0020	0.7970	0.5953	not significant
Pure Error	0.0124	5	0.0025			
Cor Total	0.6708	19				

Table 3. The summary statistics of the fitted model to the absorbance of MnO_2 nanoparticles at 350 nm. As indicated in the table the R^2 (0.9669) and the fitted R^2 (0.9370) values are closer to each other revealing that the experimentally measured and predicted values are in good agreement. Additionally, this indicates that a quadratic polynomial model can be employed to predict the reaction variables.

Std. Dev.	0.0472	R^2	0.9669
Mean	0.9501	Adjusted R^2	0.9370
C.V. %	4.9600	Predicted R^2	0.8594
		Adeq Precision	20.2439

model is appropriate, as shown in **Table 3**. The corresponding Prob. >F value of the model is less than 0.05 and is therefore statistically significant [80,81]. A, B, C, and B^2 are significant model terms, as indicated in **Table 2**. In general, the results of the statistical analysis showed that the model describes a good agreement between the independent variables and the response. A quadratic polynomial model with all variables given in coded values is presented below [82].

$$\text{Absorbance} = +1.06 - 0.0785 \times A - 0.0412 \times B + 0.1354 \times C - 0.0029 \times A \times B - 0.0521 \times A \times C + 0.0081 \times B \times C - 0.0166 \times A^2 - 0.1360 \times B^2 - 0.0023 \times C^2.$$

Figure 4a shows that the concentration to lemon extract ratio has a positive effect and thus increases the synthesis rate of the nanoparticles. As the concentration of lemon extract increases, the absorption peak of the synthesized nanoparticles also increases. However, temperature has an inverse relation to absorption; decreasing temperature increases absorption. The pH value has a stronger effect on absorption, which is in the middle range. The reference point at x = 0 shows the interaction of the variables, while the lateral positions represent the actual conditions. It can be observed that the lemon extract ratio is the most significant variable in the model. The actual and predicted values of absorption peak intensity are shown in **Figure 4b**, where the regression coefficient (R^2 = 0.9669) shows a good agreement with the proposed model.

Analysis of interaction effects: The cumulative and individual effects, as well as the joint interactions between the independent variables, were described using three-dimensional surfaces and contour plots developed from the regression mode of CCD [83]. The interaction effects between temperature and pH in terms of the intensity of the absorption peaks of the three-dimensional surface and contour plots are shown in **Figures 5a and 5b** respectively. When the temperature decreases from 60°C to 50°C and the lemon extract ratio remains at 62.5%, the absorption peak intensity increases from 0.9 to 1.1. However, at a temperature of 60°C and a pH of 4, the absorption intensity decreases to less than 0.9. In the combined effects of temperature and pH, the maximum absorption intensity of 1.1 is achieved at a temperature of 50°C

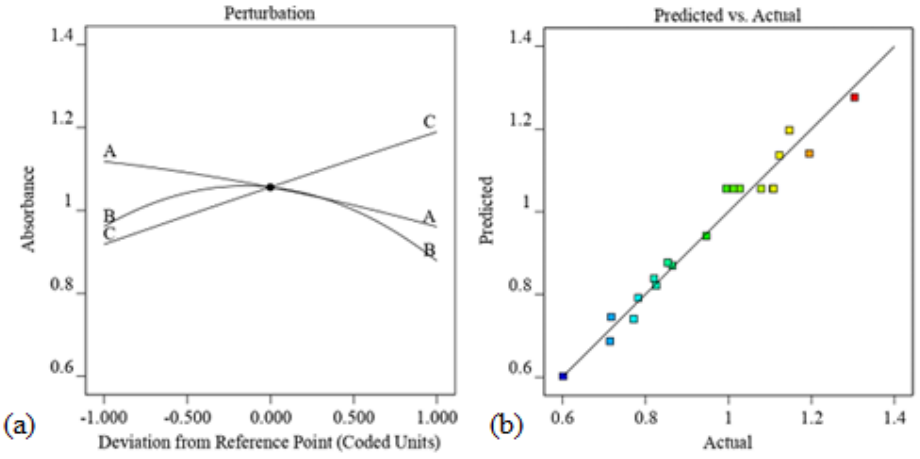

Figure 4. (**a**) displays the perturbation diagram that contrasts the effects of temperature -A, pH -B, and lemon extract ratio -C on yield; and (**b**) the expected versus actual diagram depicting the correlation between the actual and predicted values. The formation of MnO_2 nanoparticles is favored when lemon extract ratio increases, temperature decreases, and pH around the middle as shown in **Figure 4a**. The diagrams are generated using Design Expert 12 software. A regression coefficient (R^2 = 0.9669) was obtained which shows that the actual and predicted values are in good agreement as depicted in **Figure 4b**.

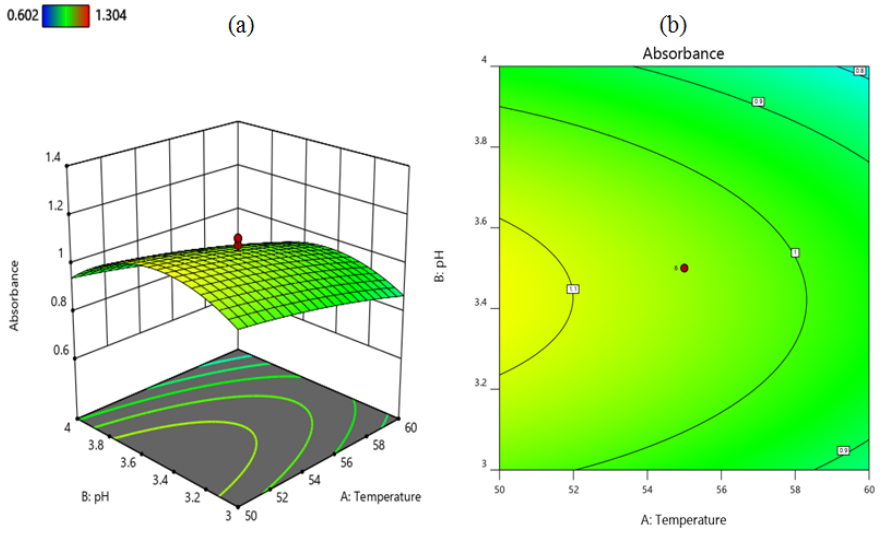

Figure 5. Three-dimensional surface (**a**) and contour plot (**b**) illustrate the interaction effect of temperature and pH on the nanoparticle synthesis. From both Figures, the interaction of temperature and pH in terms of absorbance is indicated. A lower temperature of 50°C and pH in the middle (3.4) favors the formation of the nanoparticles. This diagram was generated using Design Expert 12 software.

and a pH of about 3.4. The interaction between lemon extract ratio and temperature on absorbance is shown in **Figures 6a and 6b** as a three-dimensional surface and contour plot, respectively. When the temperature decreases from 60°C to 50°C and the lemon extract ratio increases from 50% to 75% while the pH remains at 3.5, the absorption intensity increases to 1.2. An increase in the concentration of lemon extract is correlated with an increase in the yield of MnO_2 nanoparticles. This indicates that the quantity of effective ingredients present in lemon extract exerts the greatest influence on the synthesis of MnO_2 nanoparticles. The interaction effect of pH and lemon extract ratio is depicted as three-dimensional surface and contour plots in **Figures 7a and 7b**, respectively. When the lemon extract ratio is higher, or at 75% and the pH is around

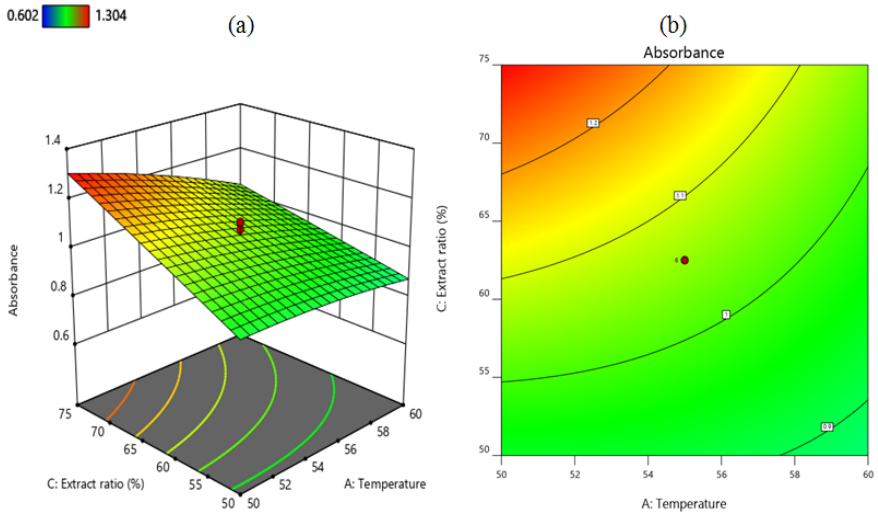

Figure 6. Three-dimensional surface (**a**) and contour plot (**b**) show the interaction effect of lemon extract ratio and temperature on the nanoparticles synthesis. A combination of a high lemon extract ratio of 75% and a low temperature of 50 °C favors the formation of nanoparticles as illustrated in both Figures. This diagram was generated using Design Expert 12 software.

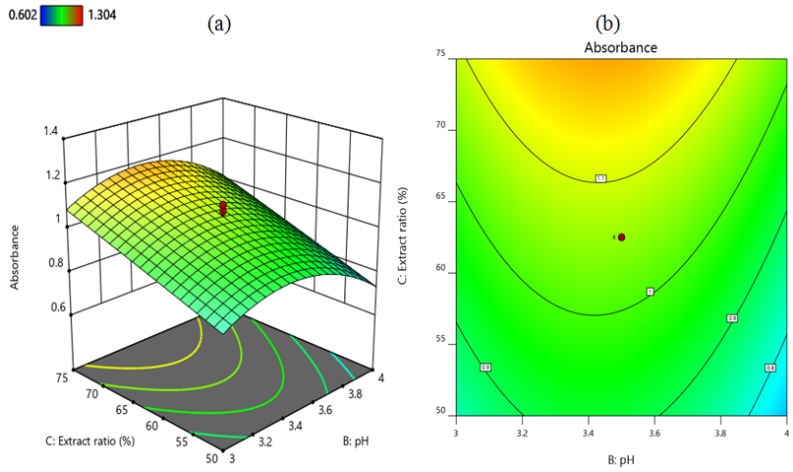

Figure 7. Three-dimensional surface (**a**) and contour plot (**b**) depict the interaction effect of lemon extract ratio and pH on the nanoparticles synthesis. A high lemon extract ratio of 75% and a pH of around 3.4 have a positive effect on the synthesis of MnO_2 nanoparticles. The diagram is generated by Design Expert 12 software.

the middle of 3.4, then the absorption peak goes up to 1.1. However, at a lower lemon extract ratio of 50% and a high pH of 4, the absorption intensity decreases to 0.8.

Optimization of the model and reaction variables: The response surface analysis may identify the set of input variables that result in the intended response, making it a practical and effective tool for optimizing experimental variables. Optimizing these variables is essential to achieve the optimal circumstances for the yield of MnO_2 nanoparticles. In this study, the lemon extract ratio, pH, and temperature were adjusted by the associated responses. The Beer-Lambert Law states that the concentration of nanoparticles and their light absorbance are directly correlated [84,85]. This law is stated as $A = \varepsilon bc$, where A is absorbance, ε is the molar extinction coefficient in units of $M^{-1}cm^{-1}$, b is the sample's path length in centimeters, and c is the concentration of nanoparticles in the solution in units of M. High absorbance values in this sense indicate a high concentration of MnO_2 nanoparticles. The response surface approach was used to find the variables that fit the best desirability associated with the concentration of nanoparticles. About 58 ideal solutions were generated by applying numerical optimization techniques to a quadratic polynomial model. The ideal values of all variables, including desirability, out of the available optimal solutions were selected by default. In this regard, the values of the variables such as temperature of 50°C, pH of 3.4, lemon extract ratio of 75%, and the maximum projected absorbance intensity of 1.304 were selected with a desirability of 1.00.

The experimental model validation: It is suggested that the predicted value is closer to that of the actual value of MnO_2 nanoparticle yield with a correlation coefficient of $R^2 = 0.9669$, as depicted in **Figure 4b**. This implies that the proposed model has been effectively developed by establishing correlations among the independent variables in the yield of MnO_2 nanoparticles. The validation was carried out under optimal conditions. To check the model validation, triplicate experiments were conducted by employing the optimal values, and the corresponding UV-visible absorption intensities were measured at a wavelength of 350 nm. Subsequently, the experimental and predicted values were compared. The resulting experimental absorption intensities were recorded as shown in **Table 4**, with an average value of

Table 4. Triplicate experiments were conducted at optimal conditions and measured absorption. The validity of the model was checked by conducting triplicate experiments of the optimal values and their corresponding UV-visible absorption intensities were recorded at a wavelength of 350 nm. The average experimental absorption intensity was 1.260 ± 0.034 and this confirmed that the model is valid with a percentage error of ± 0.034.

Run	temperature (°C)	pH	lemon extract ratio (%)	Absorption intensity at 350 nm	
				experimental	predicted
1	50	3.4	75	1.242	1.304
2	50	3.4	75	1.281	1.304
3	50	3.4	75	1.258	1.304

1.260 ± 0.034. The absorption intensities of the experimental values are found to be in line with the predicted values calculated using the model equation. The validity of the model was confirmed by the calculated percentage error of ± 0.034, which is greater than ± 0.05, indicating the closeness of the predicted and experimental values.

Applications of MnO_2 nanoparticles

MnO_2 nanoparticles offer a wide range of applications due to their diverse properties. They can absorb and intercalate ions in their structure, making them suitable for energy storage. The electrochemical capacitors developed using MnO_2 oxides offer increased power density and faster charging and discharging times. MnO_2 nanomaterials are not only good for pseudo-capacitance but also cost-effective and environmentally friendly [86]. α-MnO_2 has a wide surface area and homogenous pore dispersion, which results in the highest electrochemical capacitance as studied previously [87]. In addition, MnO_2 nanoparticles can be used as a photocatalyst for oxidizing organic compounds, including colors. MnO_2 nanoparticles can degrade methylene blue dye at a temperature of 50°C, and pH of 3.5 under sunshine irradiation, as previously reported [35]. At room temperature, MnO_2 with a crystalline tunnel-structured photochemically oxidized propanol to acetone [88]. A β-MnO_2 nanorod was employed in Fenton-type reactions in the presence of H_2O_2 to decompose methylene blue dye [89]. Furthermore, MnO_2 nanoparticles are good adsorbents in wastewater treatment. The octahedral molecular arrangement of MnO_2 nanoparticles has sieves with a large surface area, making them effective in adsorbing organic contaminants, including heavy metals, in water [90]. MnO_2 nanoparticles can be utilized with magnetic materials to enhance adsorption and are effective in wastewater treatment. These adsorbents can be regenerated by using an external magnetic field [91]. MnO_2 nanoparticles are also used in biomedical applications. They are used to detect glutathione and xenoestrogens and can also serve as non-enzymatic H_2O_2 and thiol sensors [92]. Furthermore, MnO_2 nanorods are effective in sensing potassium ions [93]. In general, MnO_2 nanoparticles have multiple functions in human life.

Conclusions

- Sustainable plant extracts improve nanoparticle synthesis with minimal environmental impact. The biosynthesis of MnO_2 nanoparticles provides a biocompatible, environmentally benign, low-cost, and time-saving technique. MnO_2 nanoparticles were synthesized by reducing manganese ions with the aid of natural lemon extract and bioactive curcumin to stabilize the nanoparticles.
- The characterizations of the nanoparticles were carried out using UV-visible spectroscopy, a field emission scanning electron microscope, and Fourier's transform infrared spectroscopy. Based on UV-visible spectroscopy analysis, the nanoparticles showed an absorption peak at a wavelength of 350 nm. The scanning electron microscope indicated that the nanoparticles were rod-shaped. Fourier's transform infrared spectroscopy detected an absorption peak at 558 cm^{-1}, which corresponded to the stretching vibration of O-Mn-O.
- The response surface methodology was employed to optimize temperature, lemon extract ratio, and pH for the biosynthesis of MnO_2 nanoparticles. The highest concentration of lemon extract was the most important variable in nanoparticle synthesis, followed by a low temperature and a pH value in the middle range. Lemon extract contains the most potent bioactive components, which contribute to the synthesis of MnO_2 nanoparticles. The formation of nanoparticles at lower temperatures can be attributed to the deactivation of the phytochemicals in plant ingredients at higher temperatures.
- MnO_2 nanoparticles are used in a variety of applications, including energy storage, photocatalysts for the oxidation of organic compounds, adsorbents in wastewater treatment, sensors, and detectors for a wide range of biomedical molecules, etc.

Declarations

Competing interest

There is no competing interest.

Funding

No funding agency supported this research.

Author contribution

Abelneh Terefe Mekuria did all the conceptualization, methodology, writing, validation, and data curation.

Acknowledgments

The author acknowledges Addis Ababa Science and Technology University for experimental works.

References

1. Kuppusamy P, Ilavenil S, Srigopalram S, Kim DH, Govindan N, Maniam GP, et al. Synthesis of bimetallic nanoparticles (Au–Ag alloy) using Commelina nudiflora L. plant extract and study its on oral pathogenic bacteria. Journal of Inorganic and Organometallic Polymers and Materials. 2017 Mar;27:562-8.

2. Alyamani AA, Albukhaty S, Aloufi S, AlMalki FA, Al-Karagoly H, Sulaiman GM. Green fabrication of zinc oxide nanoparticles using phlomis leaf extract: characterization and in vitro evaluation of cytotoxicity and antibacterial properties. Molecules. 2021 Oct 11;26(20):6140.

3. Jemilugba OT, Sakho EH, Parani S, Mavumengwana V, Oluwafemi OS. Green synthesis of silver nanoparticles using Combretum erythrophyllum leaves and its antibacterial activities, Colloid Interface Sci. Commun. 31 (2019) 100191.

4. Zinatloo-Ajabshir S, Salavati-Niasari M. Preparation of magnetically retrievable CoFe2O4@SiO2@Dy2Ce2O7 nanocomposites as novel photocatalyst for highly efficient degradation of organic contaminants. Compos Part B Eng. 2019;174:106930.

5. Zinatloo-Ajabshir S, Mousavi-Kamazani M. Recent advances in nanostructured Sn–Ln mixed-metal oxides as sunlight-activated nano photocatalyst for high-efficient removal of environmental pollutants. Ceram Int. 2021;47(17):23702-24.

6. Zinatloo-Ajabshir S, Rakhshani S, Mehrabadi Z, Farsadrooh M, Feizi-Dehnayebi M, Rakhshani S, et al. Novel rod-like [Cu(phen)2(OAc)]·PF6 complex for high-performance visible-light-driven photocatalytic degradation of hazardous organic dyes: DFT approach, Hirshfeld and fingerprint plot analysis. J Environ Manage. 2024;350:119545.

7. Zinatloo-Ajabshir S, Morassaei MS, Salavati-Niasari M. Eco-friendly synthesis of Nd2 Sn2O7 –based nanostructure materials using grape juice as green fuel as photocatalyst for the degradation of erythrosine. Compos Part B Eng. 2019;167:643-53.

8. Zinatloo-Ajabshir S, Mahmoudi-Moghaddam H, Amiri M, Akbari Javar H. A green and simple procedure to synthesize dysprosium cerate plate-like nanostructures and their application in the electrochemical sensing of mesalazine. J Mater Sci Mater Electron. 2024;35(7):1-11.

9. Herrmann JM. Heterogeneous photocatalysis: State of the art and present applications. Top Catal. 2005;34(1–4):49-65.

10. Jung T, Yun YR, Bae J, Yang S. Rapid bacteria-detection platform based on magnetophoretic concentration, dielectrophoretic separation, and impedimetric detection. Anal Chim Acta. 2021;1173:338696.

11. Anzabi Y. Biosynthesis of ZnO nanoparticles using barberry (Berberis vulgaris) extract and assessment of their physico-chemical properties and antibacterial activities. Green Process Synth. 2018;7(2):114-21.

12. Hoseinpour V, Ghaemi N. Green synthesis of manganese nanoparticles: Applications and future perspective–A review. J Photochem Photobiol B Biol. 2018;189:234-43.

13. Nguyen NTH, Tran GT, Nguyen NTT, Nguyen TTT, Nguyen DTC, Tran T Van. A critical review of the biosynthesis, properties, applications, and future outlook of green MnO2 nanoparticles. Environ Res. 2023;231(2):116262.

14. Yang R, Fan Y, Ye R, Tang Y, Cao X, Yin Z, et al. MnO2-Based Materials for Environmental Applications. Adv Mater. 2021;33(9):1-53.

15. Sisakhtnezhad S, Rahimi M, Mohammadi S. Biomedical applications of MnO2 nanomaterials as enzyme-based theranostics. Biomed Pharmacother. 2023;163:114833.

16. Dawadi S, Gupta A, Khatri M, Budhathoki B, Lamichhane G, Parajuli N. Manganese dioxide nanoparticles: synthesis, application and challenges. Bull Mater Sci. 2020;43(1):277.

17. Maleki A. Green synthesis of polyhydroquinolines via MCR using Fe3O4/SiO2-OSO3 H nanostructure catalyst and prediction of their pharmacological and biological activities by PASS. J Nanostructure Chem. 2017;7(4):309-16.

18. Jamil S, Khan SR, Sultana B, Hashmi M, Haroon M, Janjua MRSA. Synthesis of saucer shaped manganese oxide nanoparticles by co-precipitation method and the application as fuel additive. J Clust Sci. 2018;29(6):1099-106.

19. Singh P, Mijakovic I. Rowan Berries: A potential source for green synthesis of extremely monodisperse gold and silver nanoparticles and their antimicrobial property. Pharmaceutics. 2022;14(1):82.

20. Safat S, Buazar F, Albukhaty S, Matroodi S. Enhanced sunlight photocatalytic activity and biosafety of marine-driven synthesized cerium oxide nanoparticles. Sci Rep. 2021;11(1):1-11.

21. Hoseinpour V, Souri M, Ghaemi N. Green synthesis, characterization, and photocatalytic activity of manganese dioxide nanoparticles. Micro & Nano Letters. 2018;13(11):1560-3.

22. Dang T, Cheney MA, Qian S, Joo SW, Min B. A Novel Rapid One-Step Synthesis of Manganese Oxide Nanoparticles at Room Temperature Using Poly (dimethylsiloxane). Ind. Eng. Chem. Res. 2013;52(7):2750-3.

23. Kharissova O V., Dias HVR, Kharisov BI, Pérez BO, Pérez VMJ. The greener synthesis of nanoparticles. Trends Biotechnol. 2013;31(4):240-8.

24. Kumar V, Singh DK, Mohan S, Gundampati RK, Hasan SH. Photoinduced green synthesis of silver nanoparticles using aqueous extract of Physalis angulata and its antibacterial and antioxidant activity. J Environ Chem Eng. 2017;5(1):744-56.

25. Salam HA, Rajiv P, Kamaraj M, Jagadeeswaran P, Gunalan S, Sivaraj R. Plants : Green Route for Nanoparticle Synthesis. I. Res. J. Biological Sci. 2012;1(5):85-90.

26. Atrak K, Ramazani A, Taghavi Fardood S. Eco-friendly synthesis of Mg0.5Ni0.5AlxFe2-xO4 magnetic nanoparticles and study of their photocatalytic activity for degradation of direct blue 129 dye. J Photochem Photobiol A Chem. 2019;382:111942.

27. Singh Jassal P, Kaur D, Prasad R, Singh J. Green synthesis of titanium dioxide nanoparticles: Development and applications. J Agric Food Res. 2022;10:100361.

28. Bensy ADV, Christobel GJ, Muthusamy K, Alfarhan A, Anantharaman P. Green synthesis of iron nanoparticles from Ulva lactuca and bactericidal activity against enteropathogens. J King Saud Univ - Sci. 2022;34(3):101888.

29. Priya, Naveen, Kaur K, Sidhu AK. Green synthesis: An eco-friendly route for the synthesis of iron oxide nanoparticles. Front Nanotechnol. 2021;3:655062.

30. Rasheed A, Li H, Tahir MM, Mahmood A, Nawaz M, Shah AN, et al. The role of nanoparticles in plant biochemical, physiological, and molecular responses under drought stress: A review. Front Plant Sci. 2022;13:1-15.

31. Bar H, Bhui DK, Sahoo GP, Sarkar P, De SP, Misra A. Green synthesis of silver nanoparticles using latex of Jatropha curcas. Colloids Surfaces A Physicochem Eng Asp. 2009;339(1–3):134-9.

32. Hoseinpour V, Souri M, Ghaemi N, Shakeri A. Optimization of green synthesis of ZnO nanoparticles by Dittrichia graveolens (L.) aqueous extract. Heal Biotechnol Biopharma. 2017;1(2):39-49.

33. Parashar UK, Saxena PS. Bioinspired synthesis of silver nanoparticles. 2009;4(1):159-66.

34. Elizondo-Villarreal N, Verástegui-Domínguez L, Rodríguez-Batista R, Gándara-Martínez E, Alcorta-García A, Martínez-Delgado D, et al. Green synthesis of magnetic nanoparticles of iron oxide using aqueous extracts of lemon peel waste and its application in anti-corrosive coatings. Materials (Basel). 2022;15(23):8328.

35. Terefe A, Balakrishnan S. Manganese dioxide nanoparticles green synthesis using lemon and curcumin extracts and evaluation of photocatalytic activity. Mater Today Proc. 2022;62:434-41.

36. Xi W, Lu J, Qun J, Jiao B. Characterization of phenolic profile and antioxidant capacity of different fruit part from lemon (Citrus limon Burm.) cultivars. J Food Sci Technol. 2017;54(5):1108-18.

37. Del Río JA, Fuster MD, Gómez P, Porras I, García-Lidón A, Ortuño A. Citrus limon: A source of flavonoids of pharmaceutical interest. Food Chem. 2004;84(3):457-61.

38. Goodwin TW. Nature and distribution of carotenoids. Food Chem. 1980;5(1):3-13.

39. Di Matteo A, Di Rauso Simeone G, Cirillo A, Rao MA, Di Vaio C. Morphological characteristics, ascorbic acid and antioxidant activity during fruit ripening of four lemons (Citrus limon (L.) Burm. F.) cultivars. Sci Hortic (Amsterdam). 2021;276:109741.

40. Otang WM, Afolayan AJ. Antimicrobial and antioxidant efficacy of Citrus limon L. peel extracts used for skin diseases by Xhosa tribe of Amathole District, Eastern Cape, South Africa. South African J Bot. 2016;102:46-9.

41. Ehiobu JM, Idamokoro ME, Afolayan AJ. Phytochemical content and antioxidant potential of leaf extracts of Citrus limon (L.) Osbeck collected in the Eastern Cape Province, South Africa. South African J Bot. 2021;141:480-6.

42. M MH, Jayandran M, Balasubramanian V. Evaluation of antimicrobial activity of green-synthesized manganese oxide nanoparticles and comparative studies with curcumininaniline functionalized nanoform. Asian J Pharm Clin Res. 2017;10(3): 347-352

43. Veena MA, Hemanth Kumar CM, Majani SS, Munirajappa NN, Harendra B, Shivamallu C, et al. Eco-friendly synthesized manganese dioxide nanoparticles using Tridax procumbens as a potent antimicrobial and dye-degrading agent. Results Chem. 2024;7:101290.

44. Karthik P, Jose PA, Chellakannu A, Gurusamy S, Ananthappan P, Karuppathevan R, et al. Green synthesis of MnO2 nanoparticles from Psidium guajava leaf extract: Morphological characterization, photocatalytic and DNA/BSA interaction studies. Int J Biol Macromol. 2023;258(2):128869.

45. Isa EDM, Ahmad H, Rahman MBA. Optimization of synthesis parameters of mesoporous silica nanoparticles based on ionic liquid by experimental design and its application as a drug delivery agent. J Nanomater. 2019;2019: 4982054.

46. Arulkumar M, Sathishkumar P, Palvannan T. Optimization of Orange G dye adsorption by activated carbon of Thespesia populnea pods using response surface methodology. J Hazard Mater. 2011;186(1):827-34.

47. Haider S, Uddin Khan S, Najeeb J, Naeem S, Rafique H, Munir H, et al. Synthesis of cadmium oxide nanostructures by using Dalbergia sissoo for response surface methodology based photocatalytic degradation of methylene blue. J Clean Prod. 2022;365:132822.

48. Nachiyar GKV, Surendra T V., Kalaiselvi V, Rajagopal R, Kuppusamy P, Basavegowda N, et al. Box–Behnken response surface methodology design for amaranth dye degradation using gold nanoparticles. Optik (Stuttg). 2022;267:169633.

49. Mohammad Shafie N, Raja Shahriman Shah RNI, Krishnan P, Abdul Haleem N, Tan TYC. Scoping Review: Evaluation of Moringa oleifera (Lam.) for Potential Wound Healing in In Vivo Studies. Molecules. 2022; 27(17):5541.

50. Jaganyi D, Altaf M, Wekesa I. Synthesis and characterization of whisker-shaped MnO2 nanostructure at room temperature. Appl Nanosci. 2013;3(4):329-33.

51. Ahmed A, Usman M, Yu B, Ding X, Peng Q, Shen Y, et al. Efficient photocatalytic degradation of toxic Alizarin yellow R dye from industrial wastewater using biosynthesized Fe nanoparticle and study of factors affecting the degradation rate. J Photochem Photobiol B Biol. 2020;202:111682.

52. Hashem AM, Abuzeid H, Kaus M, Indris S, Ehrenberg H, Mauger A, et al. Green synthesis of nanosized manganese dioxide as a positive electrode for lithium-ion batteries using lemon juice and citrus peel. Electrochim Acta. 2018;262:74-81.

53. Manjula R, Thenmozhi M, Thilagavathi S, Srinivasan R, Kathirvel A. Green synthesis and characterization of manganese oxide nanoparticles from Gardenia resinifera leaves. Mater Today Proc. 2019;26:3559-63.

54. Gur T, Meydan I, Seckin H, Bekmezci M, Sen F. Green synthesis, characterization and bioactivity of biogenic zinc oxide nanoparticles. Environ Res. 2022;204:111897.

55. Karthik K V., Raghu A V., Reddy KR, Ravishankar R, Sangeeta M, Shetti NP, et al. Green synthesis of Cu-doped ZnO nanoparticles and its application for the photocatalytic degradation of hazardous organic pollutants. Chemosphere. 2022;287(2):132081.

56. Dong X, Shi J, Zhao J. Templated synthesis of hierarchically porous manganese oxide with a crystalline nanorod framework and its high electrochemical performance Templated synthesis of hierarchically porous manganese oxide with a crystalline nanorod framework and its high elect. J. Mater. Chem. 2007;17,855-60.

57. Jayandran M, Haneefa MM, Balasubramanian V. Green synthesis and characterization of Manganese nanoparticles using natural plant extracts and its evaluation of antimicrobial activity. J. Appl. Pharm. Sci. 2015;5(12):105-10.

58. Pourmortazavi SM, Taghdiri M, Makari V, Rahimi-Nasrabadi M. Procedure optimization for green synthesis of silver nanoparticles by aqueous extract of Eucalyptus oleosa. Spectrochim Acta - Part A Mol Biomol Spectrosc. 2015;136:1249-54.

59. Moon SA, Salunke BK, Alkotaini B, Sathiyamoorthi E, Kim BS. Biological synthesis of manganese dioxide nanoparticles by Kalopanax pictus plant extract. IET Nanobiotechnol., 2015;9(4):220-5.

60. Alaallah NJ, Abdulkareem EA, Ghaidan AF, Imran NA. Eco-friendly Approach for Silver Nanoparticles Synthesis from Lemon Extract and their Anti-oxidant, Anti-bacterial, and Anti-cancer Activities. J Turkish Chem Soc Sect A Chem. 2023;10(1):205-16.

61. Sanchez-Botero L, Herrera AP, Hinestroza JP. Oriented growth of α-MnO2 nanorods using natural extracts from grape stems and apple peels. Nanomaterials. 2017;7(5):117.

62. Dessie Y, Tadesse S, Eswaramoorthy R. Physicochemical parameter influences and their optimization on the biosynthesis of MnO2 nanoparticles using Vernonia amygdalina leaf extract. Arab J Chem. 2020;13:6472-92.

63. Miu BA, Dinischiotu A. New Green Approaches in Nanoparticles Synthesis: An Overview. Molecules 2022; 27(19):6472.

64. Prathna TC, Chandrasekaran N, Raichur AM, Mukherjee A. Biomimetic synthesis of silver nanoparticles by Citrus limon (lemon) aqueous extract and theoretical prediction of particle size. Colloids Surfaces B Biointerfaces. 2011;82(1):152-9.

65. da Silva Barros BR, do Nascimento DKD, de Araújo DRC, da Costa Batista FR, de Oliveira Lima AMN, da Cruz Filho IJ, et al. Phytochemical analysis, nutritional profile and immunostimulatory activity of aqueous extract from Malpighia emarginata DC leaves. Biocatal Agric Biotechnol. 2020;23:101442.

66. Liu Y, Heying E, Tanumihardjo SA. History, global distribution, and nutritional importance of citrus fruits. Comprehensive Reviews in Food Science and Food Safety. 2012 Nov;11(6):530-45.

67. Mudunkotuwa IA, Rupasinghe T, Wu CM, Grassian VH. Dissolution of ZnO nanoparticles at circumneutral pH: a study of size effects in the presence and absence of citric acid. Langmuir. 2012 Jan 10;28(1):396-403.

68. Khane Y, Benouis K, Albukhaty S, Sulaiman GM, Abomughaid MM, Al Ali A, et al. Green synthesis of silver nanoparticles using aqueous Citrus limon zest extract: Characterization and evaluation of their antioxidant and antimicrobial properties. Nanomaterials. 2022 Jun 10;12(12):2013.

69. Elbialy NS, Aboushoushah SF, Alshammari WW. Long-term biodistribution and toxicity of curcumin capped iron oxide nanoparticles after single-dose administration in mice. Life Sciences. 2019 Aug 1;230:76-83.

70. Qasem M, El Kurdi R, Patra D. Green synthesis of curcumin conjugated CuO nanoparticles for catalytic reduction of methylene blue. ChemistrySelect. 2020 Feb 7;5(5):1694-704.

71. Ghorbani S, Mirzaei Y, Bordbar M, Gholami A. Green Synthesis of MnO2 Nanoparticles Using Cumin Extract Composited with Hypericum Plant: Investigation of Antibacterial and Anticancer Properties. Journal of Nanostructures. 2023 Jan 1;13(1):151-8.

72. Jain S, Mehata MS. Medicinal plant leaf extract and pure flavonoid mediated green synthesis of silver nanoparticles and their enhanced antibacterial property. Scientific Reports. 2017 Nov 20;7(1):15867.

73. da Silva JD, dos Santos HC, Bento GS, Oliveira JF, de Souza Abud AK, de Fatima Gimenez I. Green synthesis of manganese dioxide (MnO2) nanoparticles produced with acerola (Malpighia emarginata) leaf extract. Materials Chemistry and Physics. 2024 Mar 1;315:128963.

74. Ramesh P, Rajendran A. Green synthesis of manganese dioxide nanoparticles: photocatalytic and antimicrobial investigations. International Journal of Environmental Analytical Chemistry. 2023 Apr 20:1-13.

75. Satpathy S, Patra A, Ahirwar B, Hussain MD. Process optimization for green synthesis of gold nanoparticles mediated by extract of Hygrophila spinosa T. Anders and their biological applications. Physica E: Low-dimensional Systems and Nanostructures. 2020 Jul 1;121:113830.

76. Souri M, Hoseinpour V, Ghaemi N, Shakeri A. Procedure optimization for green synthesis of manganese dioxide nanoparticles by Yucca gloriosa leaf extract. International Nano Letters. 2019 Mar;9:73-81.

77. Oliveira da Silva JD, dos Santos HC, Bento GS, Oliveira JFR, de Souza Abud AK, Gimenez I de F. da Silva JD, dos Santos HC, Bento GS, Oliveira JF, de Souza Abud AK, de Fatima Gimenez I. Green synthesis of manganese dioxide (MnO2) nanoparticles produced with acerola (Malpighia emarginata) leaf extract. Materials Chemistry and Physics. 2024 Mar 1;315:128963.

78. Chen X, Zhang J, Jiang X, Wang H, Kong Z, Xi J, et al. Curved surface TiO2 nanodrums coupled with MoS2 as heterojunction photocatalysts with enhancing photocatalytic activity. Materials Letters. 2018 Oct 15;229:277-80.

79. Maghsoudy N, Azar PA, Tehrani MS, Husain SW, Larijani K. Biosynthesis of Ag and Fe nanoparticles using Erodium cicutarium; study, optimization, and modeling of the antibacterial properties using response surface methodology. Journal of Nanostructure in Chemistry. 2019 Sep 1;9:203-16.

80. Hamsaveni DR, Prapulla SG, Divakar S. Response surface methodological approach for the synthesis of isobutyl isobutyrate. Process Biochemistry. 2001 May 1;36(11):1103-9.

81. Peng Y, Khaled U, Al-Rashed AA, Meer R, Goodarzi M, Sarafraz MM. Potential application of Response Surface Methodology (RSM) for the prediction and optimization of thermal conductivity of aqueous CuO (II) nanofluid: A statistical approach and experimental validation. Physica A: Statistical Mechanics and its Applications. 2020 Sep 15;554:124353.

82. Othman AM, Elsayed MA, Elshafei AM, Hassan MM. Application of response surface methodology to optimize the extracellular fungal mediated nanosilver green synthesis. Journal of Genetic Engineering and Biotechnology. 2017 Dec 1;15(2):497-504.

83. Welu KT, Beyan SM, Balakrishnan S, Admassu H. Chicken feathers based Keratin extraction process data analysis using response surface-box-Behnken design method and characterization of keratin product. Current Applied Science and Technology. 2020 Feb 4:163-77.

84. Paramelle D, Sadovoy A, Gorelik S, Free P, Hobley J, Fernig DG. A rapid method to estimate the concentration of citrate capped silver nanoparticles from UV-visible light spectra. Analyst. 2014;139(19):4855-61.

85. Shang J, Gao X. Nanoparticle counting: Towards accurate determination of the molar concentration. Chem Soc Rev. 2014;43(21):7267–78.

86. Zhang Y, Feng H, Wu X, Wang L, Zhang A, Xia T, et al. Progress of electrochemical capacitor electrode materials: A review. International Journal of Hydrogen Energy. 2009 Jun 1;34(11):4889-99.

87. Liu J, Wang W, Shen T, Zhao Z, Feng H, Cui F. One-step synthesis of noble metal/oxide nanocomposites with the tunable size of noble metal particles and their size-dependent catalytic activity. RSC Adv. 2014;4(58):30624–9.

88. Iyer A, Galindo H, Sithambaram S, King'ondu C, Chen CH, Suib SL. Nanoscale manganese oxide octahedral molecular sieves (OMS-2) as efficient photocatalysts in 2-propanol oxidation. Applied Catalysis A: General. 2010 Mar 1;375(2):295-302.

89. Cui HJ, Huang HZ, Fu ML, Yuan BL, Pearl W. Facile synthesis and catalytic properties of single crystalline β-MnO2 nanorods. Catalysis Communications. 2011 Aug 15;12(14):1339-43.

90. Hua M, Zhang S, Pan B, Zhang W, Lv L, Zhang Q. Heavy metal removal from water/wastewater by nanosized metal oxides: a review. Journal of Hazardous Materials. 2012 Apr 15;211:317-31.

91. Chen H, Chu PK, He J, Hu T, Yang M. Porous magnetic manganese oxide nanostructures: Synthesis and their application in water treatment. Journal of Colloid and Interface Science. 2011 Jul 1;359(1):68-74.

92. Julien C, Massot M, Baddour-Hadjean R, Franger S, Bach S, Pereira-Ramos JP. Raman spectra of birnessite manganese dioxides. Solid State Ionics. 2003 Apr 1;159(3-4):345-56.

93. Ahn MS, Ahmad R, Yoo JY, Hahn YB. Synthesis of manganese oxide nanorods and its application for potassium ion sensing in water. J Colloid Interface Sci. 2018;516:364-70.